A waveless two-dimensional flow in a channel against an inclined wall with surface tension effect

2007 J. Phys. A: Math. Theor. 40 14317

(http://iopscience.iop.org/1751-8121/40/47/019)

IOP Publishing Journal of Physics A: Mathematical and Theoretical

J. Phys. A: Math. Theor. **40** (2007) 14317–14328 doi:10.1088/1751-8113/40/47/019

A waveless two-dimensional flow in a channel against an inclined wall with surface tension effect

Abdelkrim Merzougui[1], **Hocine Mekias**[2] **and Fairouz Guechi**[2]

[1] Département de Mathématiques, Faculté des sciences, Université Mohamed Boudiaf, M'sila, 28000, Algeria
[2] Département de Mathématiques, Faculté des sciences, Université Farhat Abbas Sétif 19000, Algeria

E-mail: shamdadz@yahoo.fr

Received 16 April 2007, in final form 16 October 2007
Published 6 November 2007
Online at stacks.iop.org/JPhysA/40/14317

Abstract

Surface tension effect on a two-dimensional channel flow against an inclined wall is considered. The flow is assumed to be steady, irrotational, inviscid and incompressible. The effect of surface tension is taken into account and the effect of gravity is neglected. Numerical solutions are obtained via series truncation procedure. The problem is solved numerically for various values of the Weber number α and for various values of the inclination angle β between the horizontal bottom and the inclined wall.

PACS numbers: 47.15.Hg, 47.20.Dr, 47.27.Wg
Mathematics Subject Classification: 76B10, 76C05, 76M25

1. Introduction

We consider a steady two-dimensional channel flow against a wall of semi-infinite length, making an angle β with the horizontal (figure 1(a)). The fluid is assumed to be inviscid, incompressible and the flow is irrotational. If we take the symmetry of the flow with respect to the bottom wall, which is a streamline, we obtain a symmetrical jet flow impinging into an angle formed by the two semi-infinite plates (figure 1(b)). Jets impinging on walls were studied by many authors. Peng and Parker [12] considered a fluid jet impinging on an uneven wall. In their article, the authors considered different smooth geometry of the wall, symmetrical and non-symmetrical. Neglecting the gravity and the surface tension they could formulate the problem into an integral equation on the free boundary which they solved numerically. Dias, Elcrat and Trefethen [8] considered a jet emerging from a polygonal nozzle, neglecting the gravity and surface tension. Despite that the problem could theoretically be solved by the hodograph and Schwartz–Christoffel transform, but in the case where the nozzle has many corners, the Schwartz–Christoffel transform is obsolete. To remedy this mathematical

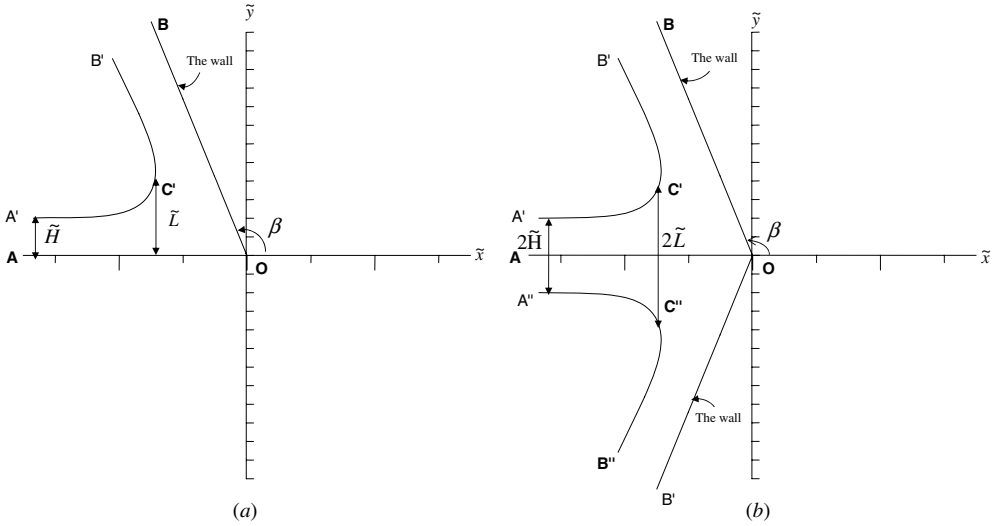

Figure 1. (*a*) Sketch of the channel flow and the coordinates. The depth of the flow far downstream $\tilde{H}$. The free surface is $A'C'B'$, β is the angle between the horizontal bottom and the inclined wall. The figure is an actual computed surface profile for $\beta = \frac{2\pi}{3}$ and $\alpha = 200$. (*b*) Sketch of a jet flow impinging into an angle of $2(\pi - \beta)$. The width of the jet at infinity is $2\tilde{H}$. The jet is assumed to be symmetrical, so that the dividing streamline is the straight line AO. The x-axis is along the streamline AO and the y-axis is vertically upward through the point O. The figure is an actual computed surface profile for $\beta = \frac{2\pi}{3}$ and the Weber number $= 200$.

limitation, the authors described an efficient mathematical procedure for computing two-dimensional ideal jets issuing from an arbitrary polygonal container. Vanden–Broeck and Tuck [14] calculated flow near the intersection of a vertical wall with a free surface taking into account gravity only and then gravity and surface tension. In the later work they presented local gravity-capillary solution near the intersection of a free surface with a wall. Similar work can be found in the study of the bow flow in which the dividing streamline can be simulated to a hard bottom. In 1993, Dias and Vanden–Broeck [9] computed via a series truncation method a model for the spray at the bow of a ship. They considered the gravity and neglected the surface tension. Because they did not neglect the gravity, the spray was modeled by a layer of water rising along the bow and following back as a jet.

In this paper, we neglect the effect of gravity but we take into account the effect of surface tension. Far upstream the velocity of the flow is a constant $\tilde{U}$ and the depth of the fluid is $\tilde{H}$.

When the effect of surface tension and gravity g is neglected, the problem has an exact solution that can be computed via the streamline method due to Kirchhoff (see, for example, [3, 4]).

If the effect of surface tension or gravity is considered, the boundary condition on the free surface is nonlinear and the problem does not have a known analytical solution. A series truncation procedure is employed to calculate the flow against a wall. This technique has been used successfully by Birkhoff and Zarantonello [4], Vanden–Broeck and Keller [15], and Dias and Vanden–Broeck [9] to calculate nonlinear free surface flow and bow flow.

As we shall see, the flow is characterized by two parameters: the angle β between the horizontal bottom and the inclined wall, and the Weber number α defined by

$$\alpha = \frac{\tilde{\rho}\tilde{U}^2\tilde{H}}{\tilde{T}}. \tag{1.1}$$

Here $\tilde{T}$ is the surface tension and $\tilde{\rho}$ is the density of the fluid.

The problem is formulated in section 2, the numerical procedure is described in section 3 and the results are discussed and presented in section 4.

2. Formulation of the problem

Let us consider the motion of a two-dimensional potential flow in a channel against an inclined wall of semi-infinite length. the inclined wall meets the horizontal bottom at the point O making an angle β. We assume that the fluid is inviscid, incompressible and the flow is irrotational and steady. Since the flow is considered to be potential the normal velocity vanishes on the rigid boundaries: the horizontal bottom and the inclined wall. Far upstream, we assume that the flow is uniform so that the velocity approaches a constant $\tilde{U}$ and the depth of the fluid tends to a constant $\tilde{H}$. The flow is limited by the free streamline $A'C'B'$, the horizontal bottom wall AO and the inclined wall OB. In the absence of gravity the main flow extends to infinity in the direction of the bottom wall far upstream and in the direction of the inclined wall OB far downstream (figure 1(*a*)). If we take the symmetry of the flow with respect to the straight streamline AO, we obtain a symmetrical jet flow impinging against two inclined walls making an angle of $2(\pi - \beta)$ between them (figure 1(*b*)). Thus, the following formulation is valid for the two problems. Our formulation is made for the flow in a channel. We choose the Cartesian coordinates such that the $\tilde{x}$-axis is along the bottom streamline and passes through the stagnation point O and the $\tilde{y}$-axis is vertically upward through the point O (considered as the origin of the axes). The angle β is counted positive in the counterclockwise from the positive axes. Since the flow is potential and is considered to be steady with the same velocity $\tilde{U}$ far upstream and downstream, it should be symmetrical with respect to the bisector of the angle AOB. Let C' denotes the intersection of the bisector of the angle AOB and the free surface, and let $(\tilde{x}_c, \tilde{y}_c)$ be its coordinates.

In this paper, we neglect the effect of gravity but we take into account the effect of surface tension. if we neglect the effects of surface tension and gravity the problem has an exact analytical solution that can be computed via hodograph transformation and free streamline theory.

Since the flow is irrotational and the fluid is incompressible, we define the complex variable $\tilde{z} = \tilde{x} + \mathrm{i}\tilde{y}$ and the complex potential function $\tilde{f} = \tilde{\phi} + \mathrm{i}\tilde{\psi}$ where $\tilde{\phi}$ is the potential function and $\tilde{\psi}$ is the stream function. Since $\tilde{\phi}$ and $\tilde{\psi}$ are conjugate solutions of Laplace's equation, $\tilde{f}(\tilde{z})$ is an analytic function of $\tilde{z}$ within the flow region. The complex conjugate velocity is given by

$$\tilde{\zeta} = \frac{\mathrm{d}\tilde{f}}{\mathrm{d}\tilde{z}} = \tilde{u}(\tilde{x}, \tilde{y}) - \mathrm{i}\tilde{v}(\tilde{x}, \tilde{y}) \tag{2.1}$$

where $\tilde{u}$ and $\tilde{v}$ are the horizontal and vertical components of the fluid velocity, respectively, and may be expressed as

$$\tilde{u} = \frac{\partial\tilde{\phi}}{\partial\tilde{x}} = \frac{\partial\tilde{\psi}}{\partial\tilde{y}}, \qquad \tilde{v} = \frac{\partial\tilde{\phi}}{\partial\tilde{y}} = -\frac{\partial\tilde{\psi}}{\partial\tilde{x}}. \tag{2.2}$$

Without loss of generality, we choose $\tilde{\psi} = 0$ on the streamline AOB and $\tilde{\phi} = 0$ at the origin O $((\tilde{x}, \tilde{y}) = (0, 0))$. The complex potential $\tilde{f}$ maps the flow domain conformally onto the infinite strip of width $\tilde{U}\tilde{H}$ as shown in figure 2.

On the free streamline (free surface) $A'C'B'$, the Bernoulli equation is to be satisfied, that is

$$\frac{1}{2}\tilde{q}^2 + \frac{\tilde{p}}{\tilde{\rho}} = C \qquad \text{on} \qquad \tilde{\psi} = \tilde{U}\tilde{H}, \quad -\infty < \tilde{\phi} < +\infty \tag{2.3}$$

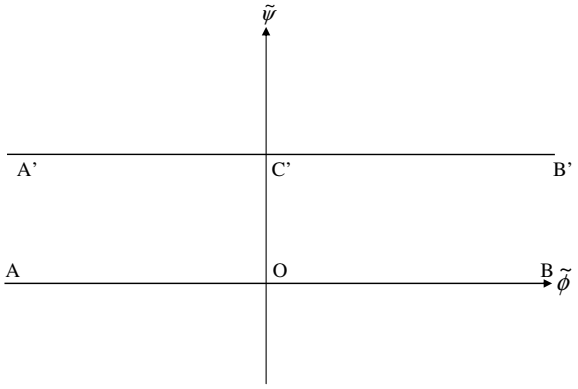

Figure 2. The complex potential f-plane, $\tilde{f} = \tilde{\phi} + \mathrm{i}\tilde{\psi}$.

where $\tilde{p}$ is the pressure of the fluid in a point on the free surface $A'C'B'$, $\tilde{\rho}$ is the density of the fluid and $\tilde{q} = \sqrt{\tilde{u}^2 + \tilde{v}^2}$ is the speed of the fluid particle on the free surface. Let $\tilde{p}_0$ be the pressure outside the fluid just above the free surface. $\tilde{p}_0$ is considered to be a constant. Since far upstream the free surface is horizontal, we have $\tilde{p} = \tilde{p}_0$. Thus, the constant C in equation (2.3) is evaluated far upstream and is given by

$$\frac{1}{2}\tilde{U}^2 + \frac{\tilde{p}_0}{\tilde{\rho}} = C.$$

A relationship between $\tilde{p}$ and $\tilde{p}_0$ is given by Laplace's capillary formula

$$\tilde{p} - \tilde{p}_0 = -\tilde{T}\tilde{K}. \tag{2.4}$$

Here $\tilde{K}$ is the curvature of the free surface and $\tilde{T}$ is the surface tension with the convention that $\tilde{K}$ is positive if the center of curvature of the free surface is inside the fluid and $\tilde{K}$ is negative otherwise.

If we substitute (2.4) into (2.3) we obtain

$$\frac{1}{2}\tilde{q}^2 - \frac{\tilde{T}}{\tilde{\rho}}\tilde{K} = \frac{1}{2}\tilde{U}^2. \tag{2.5}$$

We introduce the dimensionless variables by taking $\tilde{H}$ as the unit length and $\tilde{U}$ as the unit velocity. The dimensionless variables are given by

$$x = \frac{\tilde{x}}{\tilde{H}}, \qquad y = \frac{\tilde{y}}{\tilde{H}}, \qquad q = \frac{\tilde{q}}{\tilde{U}}, \qquad K = \tilde{H}.\tilde{R}, \qquad c = \frac{\tilde{y}_c}{\tilde{H}}, \tag{2.6}$$

the dimensionless parameter c has a special characteristic: it measures the ratio of the depth of the nearest point on the free surface to the stagnation point O to the depth of the fluid at infinity, in some papers [1, 10] this ratio is called the contraction coefficient. The dimensionless complex potential function and the dimensionless complex velocity are given by

$$f = \phi + \mathrm{i}\psi, \qquad \zeta = \frac{\mathrm{d}f}{\mathrm{d}z} = u - \mathrm{i}v.$$

Hence

$$u = \frac{\partial\phi}{\partial x} = \frac{\partial\psi}{\partial y} \qquad \text{and} \qquad v = \frac{\partial\phi}{\partial y} = -\frac{\partial\psi}{\partial x}.$$

(Here $z = x + \mathrm{i}y$, ϕ is the dimensionless potential function, ψ is the dimensionless stream function, u is the component of the dimensionless velocity in the direction of the x-axis and

v is its component in the direction of the y-axis.) In the dimensionless form, the Bernoulli boundary equation (2.5) reduces to

$$q^2 - \frac{2}{\alpha}K = 1. \tag{2.7}$$

Here α is the Weber number defined in (1.1).

The physical flow problem as formulated above can be formulated as a boundary value problem in the potential function $\phi(x, y)$:

(1) $\nabla^2\phi = 0$ in the flow domain.
(2) $\frac{\partial\phi}{\partial\eta}$=0 on the rigid boundary (the normal velocity vanishes on the rigid boundaries).
(3) $|\nabla\phi|^2 - \frac{2}{\alpha}K = 1$ on the free surface.
(4) $\phi(0, 0) = 0$.

Solving the problem in this form is very difficult especially that the nonlinear boundary condition is specified on an unknown boundary (the free surface). Instead of solving the problem in its partial differential equation form in ϕ, we take advantage of the property that for the bidimensional potential flow (as is in our problem) and if the plane in which the flow is embedded is identified to the complex plane, the complex velocity $\zeta = u - \mathrm{i}v$ and the complex potential function $f = \phi + \mathrm{i}\psi$ are analytical functions. Hence, we use all the necessary properties of analytical functions of a complex variable: integral formulation, series formulation, conform transformation, etc.

We rewrite the dimensionless complex velocity in the new variables τ and θ as

$$\zeta = u - \mathrm{i}v = \mathrm{e}^{\tau - \mathrm{i}\theta}, \tag{2.8}$$

where $\mathrm{e}^{\tau} = |\zeta|$ and θ is the angle the streamline makes with the x-axis. We seek τ and θ as functions of the variables ϕ and ψ. In these variables (ϕ, ψ) the flow domain is the strip $-\infty < \phi < +\infty$ and $0 \leqslant \psi \leqslant 1$.

Hence, equation (2.7) becomes

$$\frac{\partial\theta}{\partial\phi} = \frac{\alpha}{2}(\mathrm{e}^{\tau} - \mathrm{e}^{-\tau})\psi = 1, \qquad -\infty < \phi < \infty. \tag{2.9}$$

The kinematic condition on AO and OB yields

$$\begin{cases} \theta = 0, \psi = 0, -\infty < \phi < 0 & \text{on} \quad AO \\ \theta = \beta, \psi = 0, 0 < \phi < \infty & \text{on} \quad OB \end{cases}. \tag{2.10}$$

We shall seek $\tau - \mathrm{i}\theta$ as an analytic function of $f = \phi + \mathrm{i}\psi$ in the region $0 < \psi < 1$.

We go a step further with conformal mapping. Using the Schwartz–Christoffel transformation, we map the strip $0 < \psi < 1$ in the f-plane onto the lower half of the unit disc of an auxiliary t-plane by the transformation

$$f = \frac{2}{\pi}\log\left(\frac{1-t}{1+t}\right). \tag{2.11}$$

The stagnation point O is mapped into the origin, the points at infinity $A = A'$ and $B = B'$ correspond to the points $t = 1$ and $t = -1$, respectively. Due to the symmetry, the point C is mapped onto the point $t = -\mathrm{i}$. The solid boundary maps onto the real diameter and the free surface onto the lower half unit circle (figure 3).

In all the flow domains, the complex velocity $\zeta(t) = u - \mathrm{i}v$ is analytic except at the point O, which corresponds to $t = 0$, where the flow is inside a corner. Hence, a close study in the neighborhood of this point is to be done.

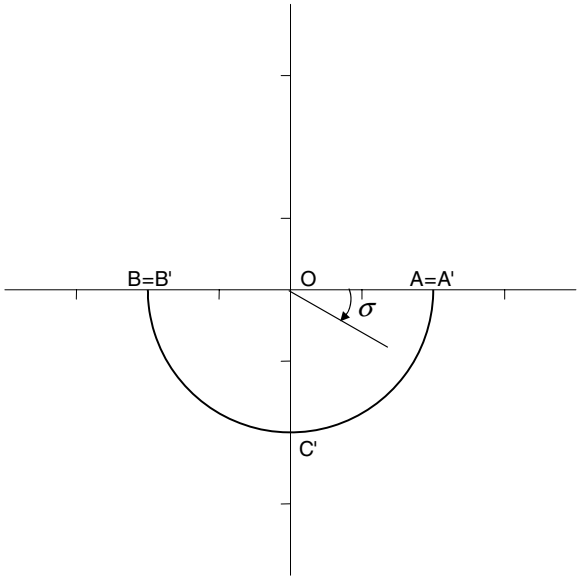

Figure 3. The complex potential t-plane.

At $t = 0$, we have a flow inside an angle of measure $\pi - \beta$, this gives the local behavior of $\zeta(t)$ as

$$\zeta = \bigcirc(t^{\frac{\beta}{\pi}}) \qquad \text{as} \quad t \longrightarrow 0. \tag{2.12}$$

Now that we know the local behavior of $\zeta(t)$ near the singularity, we seek the function $\zeta(t)$ as a series of the form

$$\zeta(t) = t^{\frac{\beta}{\pi}} \exp\left(\sum_{i=0}^{\infty} a_n t^{2n}\right). \tag{2.13}$$

The coefficients a_n are to be determined. Since (2.13) satisfies (2.12) we expect the series to converge in the lower half disc in the t-plane. The coefficients a_n are chosen to be real, so that the boundary conditions (2.10) are satisfied, i.e., $u = \cos\beta$ on OB and $v = 0$ on AO.

We use the notation $t = |t|\,\mathrm{e}^{\mathrm{i}\sigma}$ so that the points on $A'C'B'$ are given by $t = \mathrm{e}^{\mathrm{i}\sigma}$ and $-\pi < \sigma < 0$. Using (2.11), the expression (2.9) is rewritten as

$$\exp(2\tau) - \frac{\pi}{\alpha}\exp(\tau)\sin(\sigma)\left|\frac{\partial\theta}{\partial\sigma}\right| = 1. \tag{2.14}$$

Here $\tau(\sigma)$ and $\theta(\sigma)$ denote the values of τ and θ on $t = \mathrm{e}^{\mathrm{i}\sigma}$ and $-\pi < \sigma < 0$. Setting $t = \mathrm{e}^{\mathrm{i}\sigma}$ and $\zeta(t) = \mathrm{e}^{\tau - \mathrm{i}\theta}$ in (2.14) yields an equation to determine the unknowns a_n.

3. Numerical procedure

We solve the problem by truncating the infinite series in (2.13) after N terms. Introducing the N mesh points

$$\sigma_I = \frac{-\pi}{N}\left(I - \frac{1}{2}\right), \qquad I = 1, \ldots, N. \tag{3.1}$$

The N coefficients a_n are found by collocation. Using (2.14) we obtain $\tau(\sigma), \theta(\sigma)$ and $\frac{\partial\theta}{\partial\sigma}$ in terms of coefficients a_n. Upon substituting these expressions into (2.14) we obtain N nonlinear algebraic equations for the N unknowns $\{a_n\}_{n=1}^{N}$. That is, for each $\sigma(j)$, $j = 1, \ldots, N$,

$$\exp(2\tau_j) - \frac{\pi}{\alpha}\exp(\tau_j)\sin(\sigma_j)|\partial\theta_j| = 1,$$

where $\tau_j = \tau(\sigma_j)$, $\partial\theta_j = \frac{\partial\theta}{\partial\sigma}|_{\sigma=\sigma_j}$ and $\zeta(t_j) = \exp(\tau_j - \mathrm{i}\theta_j) = t_j^{\frac{\beta}{\pi}}\exp\left(\sum_{k=0}^{N} a_n t_j^{2n}\right)$ with $t_j = \mathrm{e}^{\mathrm{i}\sigma_j}$.

The Weber number α and the angle β are parameters. We solve this system by Newton method for given values of α and β.

To draw the free surface we use the identity

$$\frac{\partial x}{\partial\varphi} + \mathrm{i}\frac{\partial y}{\partial\varphi} = \frac{1}{\zeta} = \frac{1}{u - \mathrm{i}v} = \mathrm{e}^{-\tau+\mathrm{i}\theta}. \tag{3.2}$$

In the new variables σ and τ, (3.2) rewrites

$$\begin{cases} \dfrac{\partial x}{\partial\sigma} = \dfrac{2}{\pi}\exp(-\tau)\cos(\theta)\dfrac{1}{\sin(\sigma)} \\ \dfrac{\partial y}{\partial\sigma} = \dfrac{2}{\pi}\exp(-\tau)\sin(\theta)\dfrac{1}{\sin(\sigma)}. \end{cases} \tag{3.3}$$

To obtain the form of the free surface $A'C'B'$, we take advantage of the symmetry with respect to the bisector of the angle AOB. We numerically integrate the expression (3.3) in the interval $-\frac{\pi}{2} < \sigma < 0$, letting $y(N+1)$ and $x(N+1)$ be the coordinates of the point C'. Due to the symmetry of the flow with respect to the bisector of the angle AOB, we can find the relation $x(i+1) = \frac{y(i+1)}{\tan(\frac{\pi+\beta}{2})}$ for $i = 1, \ldots, N$. The Euler method was used to integrate numerically the relation (3.3).

4. Results and discussion

We use the numerical procedure described in section 3 to compute solutions of the problem for various values of the Weber number α. For fixed values of $\alpha(0 < \alpha < \infty)$ and $\beta(0 \leqslant \beta < \pi)$ the coefficients a_n were found to decrease very rapidly as n increases (table 1).

For values of α very large ($\alpha \geqslant 10^2$) (table 2), all the coefficients of the series (2.13) are zeros ($a_i = 0$ for all $i \geqslant 1$). This gives the exact solution for $(\alpha \to \infty)\zeta(t) = t^{\frac{\beta}{\pi}}$. This result was compared with the exact solution found via the hodograph transform due to Kirchhoff [3] and were found to agree exactly. In figure 4, the exact solution via the hodograph transform for $\beta = \frac{\pi}{2}$,

$$\begin{cases} x(s) = -1 - \dfrac{1}{\pi}\log\left(\dfrac{1+\sqrt{1-s}}{1-\sqrt{1-s}}\right) \\ y(s) = 1 + \dfrac{1}{\pi}\log\left(\dfrac{1+\sqrt{s}}{1-\sqrt{s}}\right), \end{cases} \tag{4.1}$$

was compared with the solution $\zeta(t) = \sqrt{t}$. The two solutions were found to be identical.

With this numerical procedure we could compute solution for the Weber number α very small. As an example for $\beta = \frac{\pi}{4}$, we could compute the solution for all $\alpha \geqslant 0.13698$. For each value of β $(0 \leqslant \beta < \pi)$ there exists a critical value α^* (α^* very small) of α such that for $\alpha < \alpha^*$ the numerical scheme ceases to converge (table 3). The free surface was smooth with

Table 1. Some values of coefficients a_n of the series (2.13) for different values of the Weber number α and for different values of the angle of inclination β.

β	α	a_1	a_5	a_{20}	a_{50}
$\frac{\pi}{4}$	0.135	-0.8505	2.0816×10^{-2}	1.7697×10^{-3}	1.8227×10^{-5}
	10	-2.3879×10^{-2}	8.7610×10^{-4}	4.0002×10^{-5}	4.1985×10^{-7}
	$\alpha \to \infty$	-4.004×10^{-21}	6.2777×10^{-21}	4.0326×10^{-21}	1.0547×10^{-21}
$\frac{\pi}{3}$	2×10^{-3}	-5.1231	2.9453×10^{-2}	2.5526×10^{-3}	2.6324×10^{-5}
	10	-3.1835×10^{-2}	1.1681×10^{-3}	5.3336×10^{-5}	5.5867×10^{-7}
	$\alpha \to \infty$	-4.004×10^{-21}	6.2777×10^{-21}	4.0326×10^{-21}	1.0547×10^{-21}
$\frac{2\pi}{3}$	3×10^{-4}	-7.6264	4.8419×10^{-2}	4.1284×10^{-3}	4.2636×10^{-5}
	10	-6.3624×10^{-2}	2.3362×10^{-3}	1.0666×10^{-4}	1.1074×10^{-6}
	$\alpha \to \infty$	-4.004×10^{-21}	6.2777×10^{-21}	4.0326×10^{-21}	1.0547×10^{-21}
$\frac{3\pi}{4}$	2×10^{-5}	-10.2719	5.2193×10^{-2}	4.4389×10^{-3}	4.5798×10^{-5}
	10	-7.1559×10^{-2}	2.6283×10^{-3}	1.1999×10^{-4}	1.2429×10^{-6}
	$\alpha \to \infty$	-4.004×10^{-21}	6.2777×10^{-21}	4.0326×10^{-21}	1.0547×10^{-21}

Table 2. Some values of coefficients a_n of the series (2.13) for different values of the Weber number $\alpha \geqslant 100$ and for different values of the angle of inclination β.

β	α	a_1	a_5	a_{10}	a_{30}	a_{45}
$\frac{\pi}{4}$	100	-2.4877×10^{-3}	8.0240×10^{-5}	1.5586×10^{-5}	1.2429×10^{-6}	2.4220×10^{-7}
	200	-1.2469×10^{-3}	3.9849×10^{-5}	7.7141×10^{-6}	6.1363×10^{-7}	1.1983×10^{-7}
	1000	-2.49882×10^{-4}	7.9269×10^{-6}	1.5300×10^{-6}	1.2146×10^{-7}	2.3986×10^{-8}
$\frac{\pi}{3}$	100	-3.3170×10^{-3}	1.0698×10^{-4}	2.0781×10^{-5}	1.6573×10^{-6}	3.2294×10^{-7}
	200	-1.6625×10^{-3}	5.3132×10^{-5}	1.0285×10^{-5}	8.1818×10^{-7}	1.5977×10^{-7}
	1000	-3.3317×10^{-4}	1.0569×10^{-5}	2.0400×10^{-6}	1.6195×10^{-7}	3.1981×10^{-8}
$\frac{\pi}{2}$	100	-4.9754×10^{-3}	1.6048×10^{-4}	3.1172×10^{-5}	2.4859×10^{-6}	4.8441×10^{-7}
	200	-2.4938×10^{-3}	7.9698×10^{-5}	1.5428×10^{-5}	1.2272×10^{-6}	2.3966×10^{-7}
	1000	-4.9976×10^{-4}	1.5853×10^{-5}	3.0601×10^{-6}	2.4293×10^{-7}	4.7972×10^{-8}
$\frac{2\pi}{3}$	100	-6.6339×10^{-3}	2.1397×10^{-4}	4.1562×10^{-5}	3.3146×10^{-6}	6.4589×10^{-7}
	200	-3.3250×10^{-3}	1.0626×10^{-4}	2.0571×10^{-5}	1.6363×10^{-6}	3.1955×10^{-7}
	1000	-6.6635×10^{-4}	2.1138×10^{-5}	4.0801×10^{-6}	3.2391×10^{-7}	6.3963×10^{-8}

Table 3. Values of the minimal Weber number α^* for different values of the angle of inclination β.

β	$\frac{\pi}{4}$	$\frac{\pi}{3}$	$\frac{\pi}{2}$	$\frac{2\pi}{3}$	$\frac{3\pi}{4}$
α^*	0.136 98	0.001 825	0.000 605	0.000 37	0.000 0302

no capillary waves even for small α. For each fixed β and as the Weber number decreases from ∞ to α^*, the shape of the free surface flattens and tends to a straight line (figures 5–7).

Figure 8 shows the variation of contraction coefficient versus the Weber number α. From the above numerical results, we conclude that for a fixed value of β ($0 \leqslant \beta < \pi$) there exist a unique solution with a smooth free surface for all $\alpha \geqslant \alpha^*$. Chapman and Vanden-Broeck [5] showed that capillary waves are exponentially small for all orders. This suggests that the series

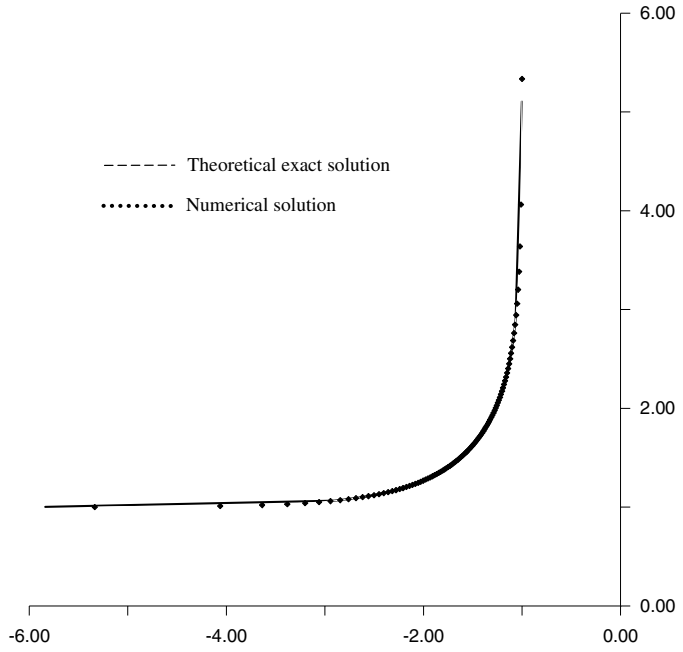

Figure 4. Comparison of the numerical free streamline shape for $\beta = \frac{\pi}{2}$ with the exact results.

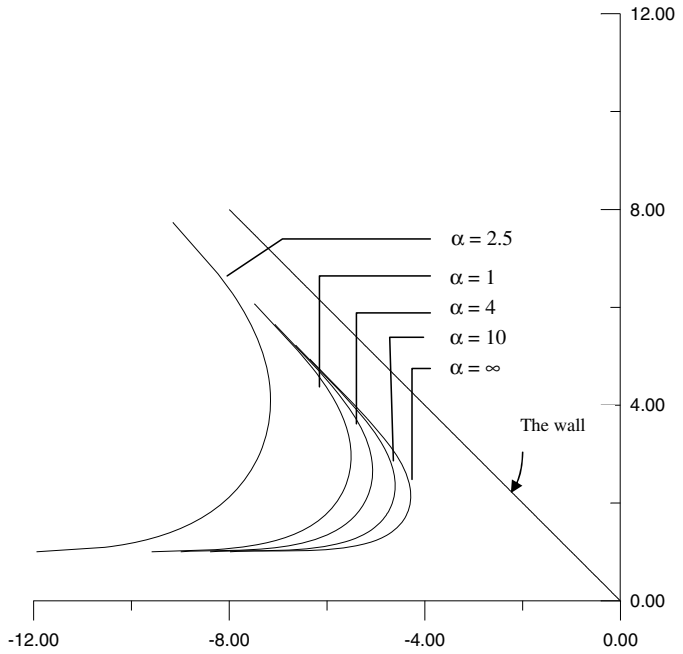

Figure 5. Free streamline shape for $\beta = \frac{3\pi}{4}$ and various Weber numbers.

formulation provides a good approximation for $\alpha \geqslant \alpha^*$. For a fixed value of β $(0 \leqslant \beta < \pi)$ and a given $\alpha < \alpha^*$ we conjecture that a solution exists with capillary surface waves. The

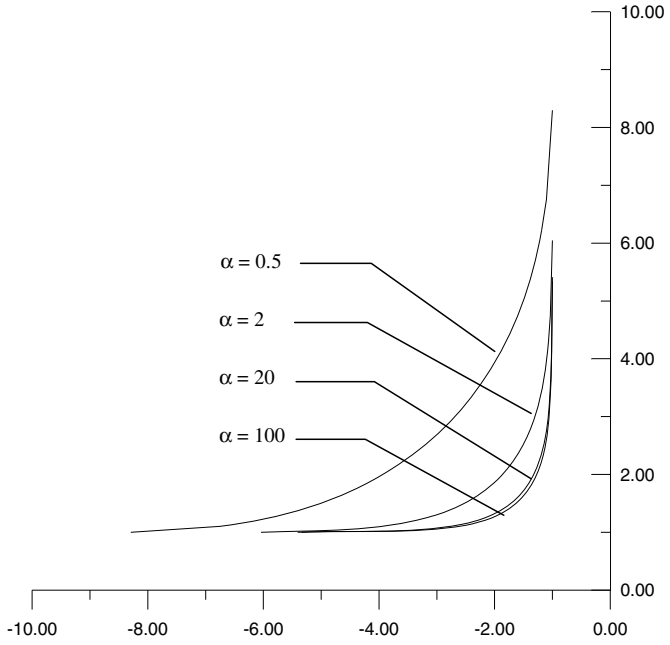

Figure 6. Free streamline shape for $\beta = \frac{\pi}{2}$ and various Weber numbers.

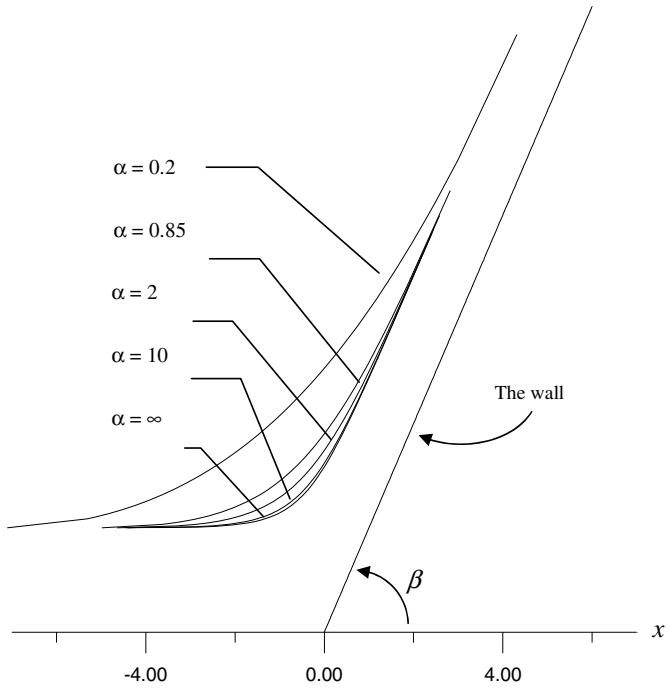

Figure 7. Free streamline shape for $\beta = \frac{\pi}{4}$ and various Weber numbers.

latter conjectured solution may be computed via an integro-differential equation which is an appropriate method for surface waves.

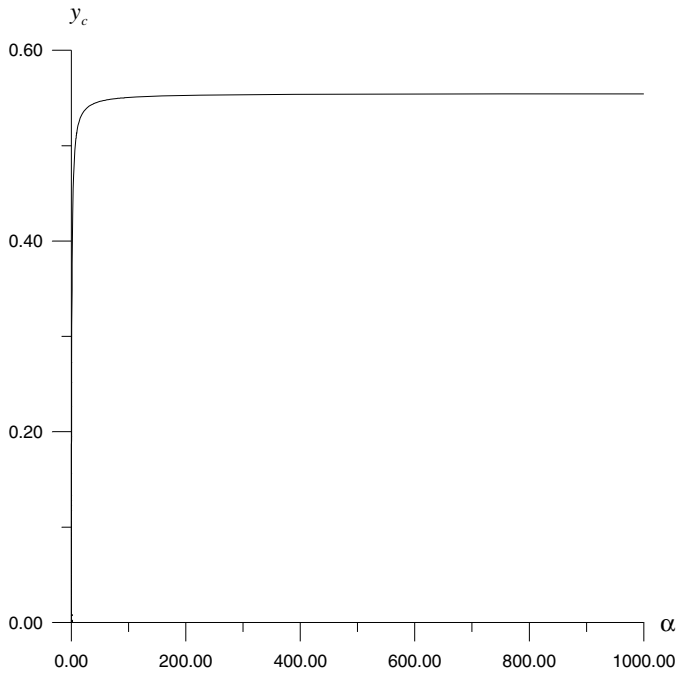

Figure 8. Coordinate of the point y_c of the point C' versus α for $\beta = \frac{3\pi}{4}$.

Table 4. Some values of coefficients a_n of the series (2.13) computed for the Weber number $\alpha = 10$ and $\beta = \frac{\pi}{2}$ with different truncation numbers.

N	a_1	a_5	a_{10}	a_{20}	a_{30}	a_{40}	a_{50}
50	-4.7739×10^2	1.7522×10^3	3.6102×10^4	8.0001×10^5	3.0030×10^5	1.1278×10^5	6.7081×10^7
80	-4.7735×10^2	1.7570×10^3	3.6571×10^4	8.5043×10^5	3.5996×10^5	1.8773×10^5	1.0554×10^5
100	-4.7735×10^2	1.7582×10^3	3.6684×10^4	8.6175×10^5	3.7210×10^5	2.0127×10^5	1.2112×10^5
120	-4.7734×10^2	1.7589×10^3	3.6747×10^4	8.6795×10^5	3.7853×10^5	2.0817×10^5	1.2870×10^5
150	-4.7734×10^2	1.7594×10^3	3.6800×10^4	8.7309×10^5	3.8376×10^5	2.1363×10^5	1.3450×10^5

The results presented here are obtained with $N = 50$. To check the sensibility with respect to the truncation number N, we computed the solution for fixed α and β for different values of N. In table 4, we give some values of the coefficients a_n computed for $\alpha = 10$ and $\beta = \pi/2$ with different truncation numbers $N = 50$, $N = 80$ and $N = 100$. Within numerical accuracy, the coefficients were found to be identical and this confirms the convergence of the series.

References

[1] Ackerberg R C and Liu T-J 1987 The effect of capillarity on the contraction coefficient of a jet emanating from a slot *Phys. Fluids* **30** 289–96
[2] Andersson C and Vanden Broeck J M 1996 Bow flows with surface tension *Proc. R. Soc.* A **452** 1–14
[3] Batchelor G K 1967 *An Introduction to Fluid Dynamics* (Cambridge: Cambridge University Press)
[4] Birkhoff G and Zarantonello E H 1957 *Jets, Wakes and Cavities* (New York: Academic)

[5] Chapman S J and Vanden-Broeck J M Exponential asymptotics and capillary waves *SIAM J. Appl. Math.* **62** 1872–98
[6] Chuang J M 2000 Numerical studies on non linear free surface flow using generalized Schwartz–Christoffel transformation *Int. J. Numer. Methods Fluids* **32** 745–72
[7] Daboussy D, Dias F and Vanden Broeck J M 1998 Gravity flows with a free surface of finite extent *Eur. J. Mech. B/Fluids* **17** 19–31
[8] Dias F, Elcrat A R and Trefethen L N 1987 Ideal jet flow in two dimensions *J. Fluid Mech.* **185** 275–88
[9] Dias F and Vanden Broeck J M 1993 Nonlinear bow flow with spray *J. Fluid Mech.* **255** 91–102
[10] Gasmi A and Mekias H 2003 The effect of surface tension on the contraction coefficient of a jet *J. Phys. A: Math. Gen.* **36** 851–62
[11] Hanna S N, Abdelmalek M N and Abd-el-Malek M B 1996 Super-critical free surface flow over a trapezoidal obstacle *J. Comput. Appl. Math.* **66** 279–91
[12] Peng W and Parker D F 1997 An ideal fluid jet impinging on an uneven wall *J. Fluid Mech.* **333** 231–55
[13] Vanden Broeck J M 1984 The effect of surface tension on the shape of the Kirchhoff jet *Phys. Fluids* **27** 1933–6
[14] Vanden Broeck J M and Tuck E O 1994 Flow near the intersection of the free surface with a vertical wall *SIAM J. Appl. Math.* **54** 1–13
[15] Vanden Broeck J M and Keller J B 1987 Weir flow *J. Fluid Mech.* **176** 283–93
[16] Vanden Broeck J M 1991 Cavitating flow of a fluid with surface tension past a circular cylinder *Phys. Fluids* A **3** 263–6